Journal of Computational Mathematics
Vol.30, No.4, 2012, 337–353.

http://www.global-sci.org/jcm
doi:10.4208/jcm.1108-m3677

EXPLICIT ERROR ESTIMATES FOR COURANT, CROUZEIX-RAVIART AND RAVIART-THOMAS FINITE ELEMENT METHODS*

Carsten Carstensen
Institut für Mathematik, Humboldt-Universität zu Berlin, Unter den Linden 6, 10099 Berlin, Germany
Department of Computational Science and Engineering, Yonsei University, 120-749 Seoul, Korea
Email: cc@math.hu-berlin.de
Joscha Gedicke
Institut für Mathematik, Humboldt-Universität zu Berlin, Unter den Linden 6, 10099 Berlin, Germany
Email: gedicke@math.hu-berlin.de
Donsub Rim
Yonsei School of Business and Department of Computational Science and Engineering, Yonsei University, 120-749 Seoul, Korea
Email: rim@yonsei.ac.kr

Abstract

The elementary analysis of this paper presents explicit expressions of the constants in the a priori error estimates for the lowest-order Courant, Crouzeix-Raviart nonconforming and Raviart-Thomas mixed finite element methods in the Poisson model problem. The three constants and their dependences on some maximal angle in the triangulation are indeed all comparable and allow accurate a priori error control.

Mathematics subject classification: 65N15, 65N12, 65N30.
Key words: Error estimates, Conforming, Nonconforming, Mixed, Finite element method.

1. Introduction

Quantitative a priori error control for the three most popular lowest-order conforming, nonconforming, and mixed 2D finite element methods (FEMs) named after Courant, Crouzeix-Raviart, and Raviart-Thomas, depicted symbolically in Figure 1.1, is one of the most fundamental questions in the numerical analysis of partial differential equations (PDEs). For the Courant FEM and the Raviart-Thomas mixed FEM (MFEM), there exist elementwise interpolation operators I and I_F such that the error analysis consists in an estimate of the Lebesgue norms in the sense of

$$\|\nabla(v - Iv)\|_{L^2(T)} \leq C(T)h_T \left\|D^2 v\right\|_{L^2(T)}$$

for some smooth function v with Hessian D^2v and the triangle T with diameter h_T. The point is that the constant $C(T)$ depends on the shape of the triangle but not on its size h_T. The textbook analysis is based on the Bramble-Hilbert lemma and so on some compact embeddings on a reference geometry [1, 2]. The transformation formula then leads to some estimate of $C(T)$ which is qualitative and can be quantified with the help of computer-justified values of some eigenvalue problem on the reference triangle, cf. e.g., [3] for a historic overview and the references quoted therein, in particular [4] for Courant and [5] for Raviart-Thomas FEM. This

* Received February 10, 2011 / Revised version received August 11, 2011 / Accepted December 14, 2011 / Published online July 6, 2012 /

paper aims at direct elementary proofs of quantitative error estimates based on the Poincaré inequality with some known constant plus elementary integration by parts.

The situation is somewhat different for the nonconforming FEMs because the local interpolation error through the natural interpolation operator I_{NC} is very sharp, even optimal by some averaging property; but the global error is also driven by the interaction with the inconsistency. The standard textbook analysis employs some Strang-Fix type argument [1, 6] which leads to two contributions and gives the reader the impression that the error analysis is even more sensitive and perhaps even the scheme is more sensitive than the other two. In Braess [1] page 111 one can even find the hint that the Crouzeix-Raviart nonconforming FEM (NCFEM) is more sensitive with respect to large second order derivatives than the other two methods.

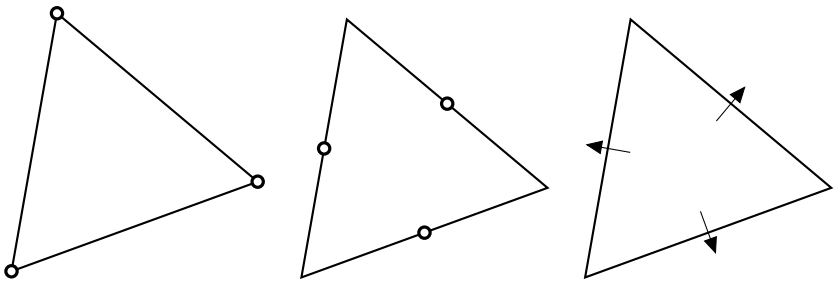

Fig. 1.1. Courant, Crouzeix-Raviart, and Raviart-Thomas FE.

This paper aims at a clarification by the comparison of the best known constants $C(T)$ for the three FEMs at hand. In fact, the constant

$$C(\alpha) := \sqrt{\frac{1/4 + 2/j_{1,1}^2}{1 - |\cos\alpha|}}, \tag{1.1}$$

for a maximal angle $0 < \alpha < \pi$ of a triangle T and the first positive root $j_{1,1}$ of the Bessel function J_1, and its maximum

$$C(\mathcal{T}) := \max_{T\in\mathcal{T}} C(\max \measuredangle T)$$

in a triangulation $\mathcal{T}$ of a 2D polygonal domain Ω play a dominant role. The main results of this paper are the explicit error estimates

$$|||u - u_C||| \le C(\mathcal{T}) \left\| h_{\mathcal{T}} D^2 u \right\|_{L^2(\Omega)}, \tag{1.2}$$

$$\|p - p_{RT}\|_{L^2(\Omega)} \le C(\mathcal{T}) \left\| h_{\mathcal{T}} Dp \right\|_{L^2(\Omega)}, \tag{1.3}$$

$$|||u - u_{CR}|||_{NC} \le \frac{1}{j_{1,1}} \operatorname{osc}(f,\mathcal{T}) + \sqrt{\frac{1}{j_{1,1}^2} + C(\mathcal{T})^2} \left\| h_{\mathcal{T}} D^2 u \right\|_{L^2(\Omega)} \tag{1.4}$$

for the Courant, Raviart-Thomas and Crouzeix-Raviart finite element approximations u_C, p_{RT} and u_{CR} in a simple Poisson model problem and the oscillations $\operatorname{osc}(f,\mathcal{T})$ defined in Section 6. In particular, the constants (which are upper bounds) have the same behaviour as the angles deteriorate with $\alpha \nearrow \pi$. The above estimate for the NCFEM displays the perturbation result for an arbitrary L^2 function f as a right-hand side in the Poisson model problem and thereby corrects and sharpens a corresponding error analysis in [7]. The technique here bypasses the

Strang-Fix argument by the direct connection of the Raviart-Thomas MFEM with the Crouzeix-Raviart NCFEM usually attributed to Marini [8, 9].

The paper is organised as follows. Section 2 presents some preliminaries and Section 3 shows the elementary interpolation estimate for the nodal interpolation operator I. The model problem and the error estimate (1.2) for the Courant finite element method is presented in Section 4. Sections 5 and 6 present the error estimates for the Raviart-Thomas MFEM (1.3) and the Crouzeix-Raviart NCFEM (1.4).

The contents of this paper reflects the way, finite element methods are taught by the first author over the years at the universities in Kiel, Vienna, Berlin, Budapest, and Seoul as well as in his summer schools in Cape Town, Beijing, Mumbai and on Goa. They seem to be optimal in the class of arguments and offer some quantitative insight with surprisingly little effort.

Throughout this paper, standard notation on Lebesgue and Sobolev spaces is employed. The Lebesgue integral reads $\int$, the integral mean $⨍$, norms $|||\cdot||| := \|\nabla\cdot\|_{L^2(\Omega)}$, $|||\cdot|||_{NC} := \|\nabla_{NC}\cdot\|_{L^2(\Omega)}$ with piecewise gradient $(\nabla_{NC}\,\cdot)|_T := \nabla(\cdot|_T)$ for all $T \in \mathcal{T}$, and $|\cdot|$ denotes the measure as the area $|T|$ of the triangle T and the length $|E|$ of an edge E.

2. Elementary Preliminaries

This section is devoted to some preliminaries for the interpolation error estimates. One is a Poincaré-Friedrichs type estimate, which follows from the well known trace identity and another is some transformation stability in the plane. Figure 2.1 displays the geometry of a triangle in the subsequent two lemmas.

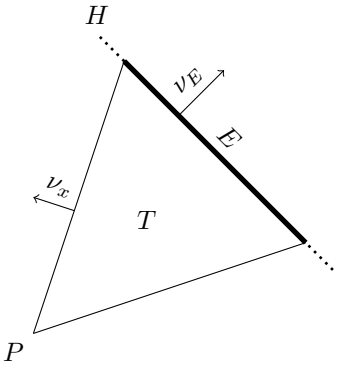

Fig. 2.1. Geometry of the triangle T from Lemma 2.1 and Lemma 2.2.

Lemma 2.1 (Trace Identity) *Let $f \in W^{1,1}(T)$ on the triangle $T = \mathrm{conv}(\{P\} \cup E)$ with vertex P and opposite edge E. Then it holds*

$$⨍_E f\,ds - ⨍_T f\,dx = \frac{1}{2} ⨍_T (x-P)\cdot\nabla f(x)\,dx.$$

Proof. Set $g(x) := (x-P)f(x)$ for all $x \in T$ and observe

$$(x-P)\cdot\nu_E = \mathrm{dist}(P,H) \quad \text{for} \quad x \in E \subset H$$

for the line H from Figure 2.1 that enlarges E. For x on one of the two other edges, $x - P$ is parallel to that edge. Hence, the unit normal ν along ∂T satisfies

$$(x - P) \perp \nu(x) \quad \text{for} \quad x \in \partial T \setminus E.$$

Therefore, the Gauss divergence theorem leads to

$$\int_T \operatorname{div} g(x)\, dx = \int_{\partial T} g(x) \cdot \nu(x)\, ds_x = \int_E f(x)\, (x - P) \cdot \nu_E\, ds_x = \operatorname{dist}(P, H) \int_E f\, ds\ .$$

This and the product rule

$$\operatorname{div} g(x) = 2f(x) + \nabla f(x) \cdot (x - P)$$

prove the assertion. □

The classical Poincaré constant of Payne-Weinberger [10] has recently been improved from $1/\pi$ (for all convex domains) to the optimal value $1/j_{1,1}$ (for triangles), where $j_{1,1} \approx 3.83170597$ denotes the first positive root of the Bessel function J_1.

Theorem 2.1 (Poincaré Inequality on Triangles [11]) *For all $f \in H^1(T)$ on a triangle T it holds*

$$\left\| f - \fint_T f(x)dx \right\|_{L^2(T)} \leq h_T/j_{1,1}\, |f|_{H^1(T)}. \tag{2.1}$$

Lemma 2.2 (Poincaré-Friedrichs Inequality) *Let $f \in H^1(T)$ satisfy $\int_E f\, ds = 0$ on the triangle $T = \operatorname{conv}(\{P\} \cup E)$ with an edge E opposite to the vertex P. Then it holds*

$$\|f\|_{L^2(T)} \leq \sqrt{\max_{x \in E} |P - x|^2 /8 + h_T^2/j_{1,1}^2}\ |f|_{H^1(T)}\ .$$

Proof. The theorem of Pythagoras for $a := f - \fint_T f(x)dx$ and $b := \fint_T f(x)dx$ reads

$$\|f\|_{L^2(T)}^2 = \|a + b\|_{L^2(T)}^2 = \|a\|_{L^2(T)}^2 + \|b\|_{L^2(T)}^2\,.$$

The Poincaré inequality (2.1) gives

$$\|a\|_{L^2(T)} = \left\| f - \fint_T f(x)dx \right\|_{L^2(T)} \leq h_T/j_{1,1}\, |f|_{H^1(T)}.$$

The trace identity from Lemma 2.1 with $\fint_E f\, ds = 0$ leads to

$$|T||b| = \Big| \int_T f(x)\, dx \Big| = \frac{1}{2} \Big| \int_T (x - P) \cdot \nabla f(x)\, dx \Big| \leq \frac{1}{2}\, \|\bullet - P\|_{L^2(T)}\, |f|_{H^1(T)}.$$

With polar coordinates (r, φ) and the notation for $|x - P| =: r$ and $\alpha < \varphi < \beta$ with some distance $0 < \delta(\varphi) \leq \max_{x \in E} |P - x|$ of P to E, one deduces

$$\begin{aligned} \|x - P\|_{L^2(T)}^2 &= \int_\alpha^\beta \int_0^{\delta(\varphi)} r^2 r\, dr\, d\varphi = \int_\alpha^\beta \delta(\varphi)^4/4\, d\varphi \\ &\leq \max_{x \in E} |P - x|^2\, /2 \int_0^\beta \int_0^{\delta(\varphi)} r\, dr\, d\varphi = |T| \max_{x \in E} |P - x|^2\, /2\,. \end{aligned}$$

This results in the bound

$$|b| = \left| \fint_T f(x)\,dx \right| \le 2^{-3/2}|T|^{-1/2} \max_{x\in E} |P-x|\,|f|_{H^1(T)}.$$

The preceding two estimates control the two terms a and b of the above Pythagoras identity and so prove

$$\begin{aligned} ||f||^2_{L^2(T)} &\le h_T^2/j_{1,1}^2\,|f|^2_{H^1(T)} + \max_{x\in E} |P-x|^2/8\,|f|^2_{H^1(T)} \\ &= \left(\max_{x\in E} |P-x|^2/8 + h_T^2/j_{1,1}^2 \right)\,|f|^2_{H^1(T)}. \end{aligned}$$ □

The following inequality compares the Euclidean length $|a|$ of a vector a in the plane with a second metric $\sqrt{(a\cdot\nu)^2+(a\cdot\mu)^2}$ given by the two projections $a\cdot\nu$ and $a\cdot\mu$.

Lemma 2.3 (Transformation Stability) *For linearly independent unit vectors ν and μ in $\mathbb{R}^2$, it holds*

$$\min_{a\in\mathbb{R}^2\setminus\{0\}} \frac{(a\cdot\nu)^2+(a\cdot\mu)^2}{|a|^2} = 1-|\nu\cdot\mu|.$$

Proof. Let $a=\alpha\nu+\beta\mu$ for real α and β with $\alpha^2+\beta^2=1$. Set $\gamma:=\nu\cdot\mu$ and $|\nu|=1=|\mu|$. Then $-1\le 2\alpha\beta\le 1$ and so

$$0\le (1+|\gamma|)(|\gamma|+2\alpha\beta\gamma).$$

This is equivalent to

$$-(1+|\gamma|)\,2\alpha\beta\gamma \le \gamma^2+|\gamma|.$$

Add $1-|\gamma|+4\alpha\beta\gamma$ on both sides to prove

$$LHS := (1-|\gamma|)(1+2\alpha\beta\gamma) = 1+2\alpha\beta\gamma-|\gamma|2\alpha\beta\gamma-|\gamma| \le 1+\gamma^2+4\alpha\beta\gamma =: RHS.$$

Direct calculations show

$$|a|^2 = \alpha^2+\beta^2+2\alpha\beta\gamma = 1+2\alpha\beta\gamma = LHS/(1-|\gamma|)$$

as well as $a\cdot\nu=\alpha+\beta\gamma$ and $a\cdot\mu=\beta+\alpha\gamma$. Therefore,

$$(a\cdot\nu)^2+(a\cdot\mu)^2 = (\alpha+\beta\gamma)^2+(\beta+\alpha\gamma)^2 = 1+\gamma^2+4\alpha\beta\gamma = RHS.$$

Altogether this proves

$$(1-|\gamma|)|a|^2 \le (a\cdot\nu)^2+(a\cdot\mu)^2 \text{ for all } a\in\mathbb{R}^2\ .$$

This shows that the left-hand side in the assertion is in fact larger than or equal to $1-|\gamma|$. Equality and attainment of the minimum follows with the choice

$$(\alpha,\beta) = \frac{1}{\sqrt{2}}(\pm 1,1) \quad \text{for } \pm\gamma\le 0$$

plus direct calculations. This concludes the proof. □

3. Nodal Interpolation Error Estimate

This section presents the nodal interpolation error estimates in an abstract form on a triangle with focus on explicit constants and then compares with the estimate from [3]. Recall the expression $C(\alpha)$ from (1.1) for any angle $0 < \alpha < \pi$ of a triangle T which is preferably chosen as $C(\max \measuredangle T)$.

Theorem 3.1 (Interpolation Error Estimate) *Let $v \in H^2(T)$ with $v(A) = v(B) = v(C) = 0$ on the triangle $T = conv\{A, B, C\}$, with vertices A, B, C, diameter h_T, and some interior angle $0 < \alpha < \pi$. Then it holds*

$$\|\nabla v\|_{L^2(T)} \leq C(\alpha)\ h_T \left\|D^2 v\right\|_{L^2(T)}.$$

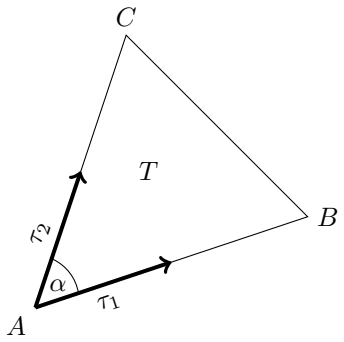

Fig. 3.1. Geometry in Theorem 3.1.

Proof. Figure 3.1 displays two unit vectors $\tau_1 = \nu$ and $\tau_2 = \mu$ along the two sides of the angle α with $|\gamma| := |\tau_1 \cdot \tau_2| = |\cos\alpha|$. Lemma 2.3 for $a := \nabla v(x)$ and $f_j := \tau_j \cdot \nabla v(x)$ plus integration over T show

$$(1 - |\gamma|) \int_T |\nabla v(x)|^2\, dx \leq \int_T \left(f_1(x)^2 + f_2(x)^2\right)\, dx.$$

Lemma 2.2 proves

$$\int_T \left(f_1(x)^2 + f_2(x)^2\right) dx \leq \max\{|A-B|^2, |A-C|^2\}/8 + h_T^2/j_{1,1}^2 \left(|f_1|^2_{H^1(T)} + |f_2|^2_{H^1(T)}\right).$$

Since $|\tau_j| = 1$ it holds for all $x \in T$ and $j, k = 1, 2$ that

$$\frac{\partial f_j}{\partial x_k}(x) = \frac{\partial}{\partial x_k} \nabla v(x) \cdot \tau_j \leq \sqrt{\sum_{\ell=1}^{2} \left|\frac{\partial^2 v(x)}{\partial x_k \partial x_\ell}\right|^2}.$$

This and

$$|f_j|^2_{H^1(T)} = \|\partial f_j/\partial x_1\|^2_{L^2(T)} + \|\partial f_j/\partial x_2\|^2_{L^2(T)}$$

for $j = 1, 2$ (which eventually results in the factor 2) lead to

$$\begin{aligned} |v|^2_{H^1(T)} &\leq \frac{1/4 + 2/j_{1,1}^2}{1 - |\cos\alpha|}\ h_T^2 \int_T \left(\left|\frac{\partial^2 v}{\partial x_1^2}\right|^2 + 2\left|\frac{\partial^2 v}{\partial x_1 x_2}\right|^2 + \left|\frac{\partial^2 v}{\partial x_2^2}\right|^2\right) dx \\ &= \frac{1/4 + 2/j_{1,1}^2}{1 - |\cos\alpha|}\ h_T^2 |v|^2_{H^2(T)} = C(\alpha)^2 h_T^2 |v|^2_{H^2(T)}. \end{aligned}$$

□

The following example illustrates how the estimate has to deteriorate as $\alpha \nearrow \pi$ and why it stays bounded under the maximal angle condition.

Example 3.1 (Maximal Angle Condition) *Given any $0 < \delta \leq 1$, consider the triangles T_1 and T_2 defined in Figure 3.2 with vertices $\mathcal{N}(T_1)$ and $\mathcal{N}(T_2)$. The point is that T_2 has some largest angle $\alpha = \pi/2$ while that of T_1 is $\alpha = 2\arctan(1/\delta)$ and this tends to π as δ tends to zero. The smooth function $v(x_1, x_2) = 1 - x_1^2$ has the nodal interpolation $Iv(x_1, x_2) = x_2/\delta$ on T_1 and one calculates*

$$\|\partial(v - Iv)/\partial x_2\|^2_{L^2(T_1)} = 1/\delta \leq \|\nabla(v - Iv)\|^2_{L^2(T_1)} \text{ for } \left\|D^2 v\right\|^2_{L^2(T_1)} = 4\delta\,.$$

Theorem 3.1 applies to the interpolation error $v - Iv$ as it vanishes at the vertices of T_1. This shows

$$Q(v) := \frac{\|\nabla(v - Iv)\|_{L^2(T_1)}}{h_{T_1}\,\|D^2 v\|_{L^2(T_1)}} \leq C(\alpha)\,.$$

Elementary trigonometric considerations show

$$(1 - |\cos\alpha|)^{-1} = (1 + \delta^2)/(2\delta^2) \leq \delta^{-2}.$$

Hence, the lower and upper bounds show the same asymptotic behaviour

$$(4\delta)^{-1} \leq Q(v) \leq \delta^{-1}\sqrt{1/4 + 2/j_{1,1}^2} \quad \text{as } \delta \searrow 0.$$

In other words, the degeneracy of $C(\alpha) \to \infty$ is sharp in the sense that

$$\sup_{\substack{v \in H^2(T_1)\setminus\{0\} \\ v = 0 \text{ at } \mathcal{N}(T_1)}} Q(v) \propto (1 - |\cos\alpha|)^{-1/2} \quad \text{as} \quad \alpha \nearrow \pi\,.$$

To illustrate the difference to the triangle T_2 with right angle $\alpha = \pi/2$, note that

$$C(\pi/2) = \sqrt{1/4 + 2/j_{1,1}^2} \approx 0.6215$$

is bounded independently of $\delta \searrow 0$. □

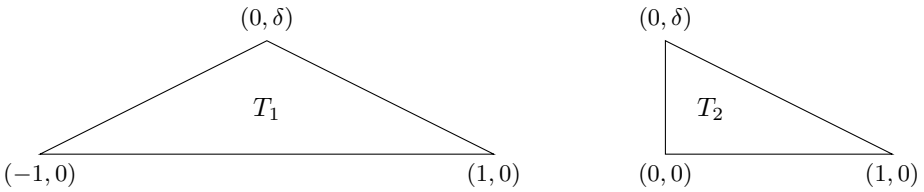

Fig. 3.2. The triangles T_1 and T_2 from Example 3.1.

The search of an optimal bound the error estimate of Theorem 3.1 can also be posed as an eigenvalue problem with the Rayleigh quotient

$$RQ(v) := \|\nabla v\|^2_{L^2(T)} \,/\, \left\|D^2 v\right\|^2_{L^2(T)} \quad \text{for } v \in H^2(T) \text{ with } v = 0 \text{ on } \mathcal{N}(T).$$

Theorem 3.1 leads to an upper bound of the first eigenvalue of this eigenvalue problem with an elementary proof. The value $C_3 = 0.489$ is known for a right isosceles triangle T from [12–14].

Remark 3.1. [Comparison with [3]] The reference [3] discusses a valid upper bound for the constant

$$C_3(T)^2 := \sup_{\substack{v\in H^2(T)\setminus\{0\}\\ v=0 \text{ at } \mathcal{N}(T)}} RQ(v) \le C(\alpha)^2 h_T^2,$$

for a triangle T with maximal angle α and diameter $h_T = \operatorname{diam}(T)$. Based on some transformation arguments, this constant has been computed and empirically studied in [3] and formerly in [12–14] with the numerical value $C_3(T_{\mathrm{ref}}) = 0.489$ on the reference triangle $T_{\mathrm{ref}} = \operatorname{conv}\{(0,0),(0,1),(1,0)\}$. Justified by computer-simulations, the bound of [3] leads to

$$C_3(T) \le \frac{1+|\cos\alpha|}{\sqrt{2}\sqrt{1-|\cos\alpha|}} \frac{C_3(T_{\mathrm{ref}})}{\sqrt{1-\cos\alpha}}\, h_T\,. \tag{3.1}$$

(The reader is warned that the notation in [3] is different and does not involve the maximum length h_T but the second largest one and there is another parameter which is maximized here in (3.1) for simplicity.) Figure 3.3 compares the upper bound in (3.1) for $C_3(T)$ and the bound $C(\alpha)$ as a function of the angle α in the range $\pi/3 \le \alpha < \pi$. Notice that an equilateral triangle T with $\alpha = \pi/3$ shows

$$C(\alpha) = 0.8789 < C_3(T) = 1.0373$$

and the bound of Theorem 3.1 is even sharper than that of [3]. This is not a contradiction because the transformation in [3] leads to some upper bound. The overall conclusion from Figure 3.3 is that the two bounds are comparable; one is with an elementary proof, while the other is justified by numerical calculations. □

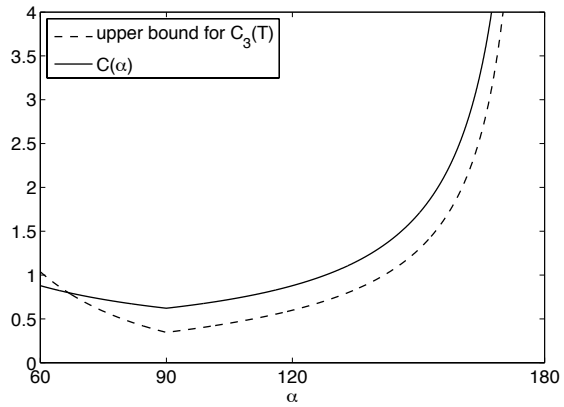

Fig. 3.3. Comparison of the constant $C(\alpha)$ and the upper bound (3.1) for $C_3(T)$.

4. Courant FEM

This section is devoted to the simplest model problem for second-order elliptic PDEs and its most elementary first-order conforming discretisation.

4.1. Poisson model problem

Given a right-hand side $f \in L^2(\Omega)$ on a bounded Lipschitz domain $\Omega \subset \mathbb{R}^2$ with polygonal boundary $\partial\Omega$, the strong form of the Poisson model problem reads: seek $u \in C(\bar{\Omega}) \cap H^2_{loc}(\Omega)$ such that

$$-\Delta u = f \text{ in } \Omega \quad \text{and} \quad u = 0 \text{ along } \partial\Omega. \tag{4.1}$$

The formally equivalent weak formulation utilizes the scalar product and the linear and bounded functional

$$a(u,v) := \int_\Omega \nabla u \cdot \nabla v \; dx \qquad \text{and} \qquad F(v) := \int_\Omega fv \; dx \qquad \text{for } u, v \in V := H^1_0(\Omega)$$

in the Hilbert space $H^1_0(\Omega)$ of Lebesgue measurable functions in $L^2(\Omega)$ with a weak gradient in $L^2(\Omega;\mathbb{R}^2)$. The weak form seeks the Riesz representative u of F within the Hilbert space V, namely $u \in V$ with

$$a(u,v) = F(v) \quad \text{for all } v \in V \; . \tag{4.2}$$

Elliptic regularity leads to $u \in H^2_{loc}(\Omega) \cap H^{1+s}(\Omega)$ for some $1/2 < s \leq 1$ with $s = 1$ for convex domains [15, 16].

4.2. Regular triangulation

A *regular triangulation* $\mathcal{T}$ of Ω (in the sense of Ciarlet) into triangles is a finite set of closed triangles T of positive area $|T|$ such that

$$\bigcup \mathcal{T} := \bigcup_{T \in \mathcal{T}} T = \overline{\Omega}$$

and any two distinct triangles T_1 and T_2 in $\mathcal{T}$ with $T_1 \cap T_2 \neq \emptyset$ share exactly one vertex z or have one edge E in common. The *set of all edges* of a triangle T is denoted by $\mathcal{E}(T)$, the *set of vertices* of T is denoted by $\mathcal{N}(T)$. The set of all edges resp. nodes is written as

$$\mathcal{E} := \bigcup_{T \in \mathcal{T}} \mathcal{E}(T) \quad \text{and} \quad \mathcal{N} := \bigcup_{T \in \mathcal{T}} \mathcal{N}(T).$$

Let $\mathrm{mid}(\mathcal{E}) := \{\mathrm{mid}(E) \,|\, E \in \mathcal{E}\}$ be the set of midpoints of the edges. The piecewise constant weight $h_{\mathcal{T}} \in \mathcal{P}_0(\mathcal{T})$ is the local mesh-size,

$$h_{\mathcal{T}}|_T := h_T := \mathrm{diam}(T) \quad \text{for all } T \in \mathcal{T}.$$

4.3. Courant FEM

For a regular triangulation $\mathcal{T}$ of Ω and $k \in \mathbb{N}_0$ define the finite element spaces

$$\begin{aligned} P_k(T) &:= \{\text{polynomial on } T \text{ with degree} \leq k\} \; , \\ P_k(\mathcal{T}) &:= \{v \in L^2(\Omega) \,|\, \forall T \in \mathcal{T}, v|_T \in P_k(T)\} \; , \\ V_C(\mathcal{T}) &:= \mathcal{C}_0(\Omega) \cap P_k(\mathcal{T}) \; . \end{aligned}$$

The *nodal basis function* $\varphi_z \in \mathcal{C}(\Omega) \cap P_1(\mathcal{T})$ is defined by $\varphi_z(z) = 1$ and $\varphi_z(y) = 0$ for $z \in \mathcal{N}$ and all other nodes $y \in \mathcal{N} \setminus \{z\}$. The *nodal interpolant* is the operator

$$I : C(\overline{\Omega}) \to V_C(\mathcal{T}), \quad v \mapsto \sum_{z \in \mathcal{N}} v(x)\varphi_z(x).$$

The Galerkin discretisation replaces $H^1_0(\Omega)$ by the finite element space $V_C(\mathcal{T})$: seek $u_C \in V_C$ with

$$a(u_C, v_C) = F(v_C) \quad \text{for all} \quad v_C \in V_C. \tag{4.3}$$

The following immediate consequence of Theorem 3.1 and the well-known optimality of u_C implies (1.2).

Corollary 4.1. *The Courant FEM solution u_C on Ω of the Poisson model problem* (4.1) *satisfies*

$$|||u - u_C||| \le |||u - Iu||| \le C(\mathcal{T}) \left\| h_{\mathcal{T}} D^2 u \right\|_{L^2(\Omega)}.$$

Proof. The first inequality follows from Galerkin orthogonality and the second from Theorem 3.1 because $u - Iu$ vanishes at all nodes. □

4.4. Numerical example

Consider the Poisson model problem (4.1) with

$$f(x, y) = 4 - 2x^2 - 2y^2 \quad \text{for } (x, y) \in \Omega := (-1, 1)^2$$

and exact solution $u(x, y) = (1-x^2)(1-y^2)$. The sequence of uniform criss triangulations $(\mathcal{T}_\ell)_\ell$ of the unit square Ω is generated by uniform refinements of Ω into squares divided along the diagonal parallel to the main diagonal. Table 4.1 shows the errors computed with Matlab [17] for different levels ℓ with mesh-sizes $h_{\mathcal{T}_\ell} = \sqrt{2}/2^\ell$ and efficiency indices

$$EI := (C(\mathcal{T}_\ell) \left\| h_{\mathcal{T}_\ell} D^2 u \right\|_{L^2(\mathcal{T}_\ell)}) / |||u - u_C|||.$$

Table 4.1: Numerical results for Courant FEM.

ℓ	1	2	3	4	5
$\|\|\|u - u_C\|\|\|$	1.70981192	0.94119129	0.48268572	0.24290612	0.12165024
$\|\|\|u - Iu\|\|\|$	1.73845397	0.94721815	0.48353983	0.24301633	0.12166412
EI	2.87527872	2.61168258	2.54626645	2.52987950	2.52577899

5. Raviart-Thomas MFEM

This section is devoted to the error analysis of the Raviart-Thomas mixed finite element method. The first subsection presents the key argument.

5.1. Fortin interpolation error estimate

This subsection is devoted to the error analysis in simplified notation. The Fortin interpolation will be defined in Subsection 5.2 below.

Theorem 5.1 (Fortin Interpolation Error Estimate) *Let $q \in H^1(T;\mathbb{R}^2)$ on the triangle $T = conv\{P_1, P_2, P_3\}$ with maximal angle α with*

$$\int_E q \cdot \nu_E \, ds = 0 \quad \textit{for all } E \in \mathcal{E}(T).$$

Then it holds

$$\|q\|_{L^2(T)} \leq C(\alpha) \, \|h_T \, Dq\|_{L^2(T)} \, .$$

Proof. Let E_1, E_2, E_3 be the edges of T and ν_1, ν_2, ν_3 corresponding exterior unit normal vectors. Then

$$f_j := q \cdot \nu_j \in H^1(T) \;\text{ satisfies }\; \int_{E_j} f_j \, ds = 0$$

for any $j = 1, 2, 3$. Lemma 2.2 implies

$$\|f_j\|_{L^2(T)} \leq h_T \sqrt{1/8 + 1/j_{1,1}^2} \, |f_j|_{H^1(T)} \, .$$

Suppose that the maximum angle α of T is at P_3 with neighbouring edges E_1 and E_2. Lemma 2.3 implies for $\nu = \nu_1$ and $\mu = \nu_2$ with $|\nu_1 \cdot \nu_2| = |\cos\alpha|$ that

$$(1 - |\cos\alpha|) \, \|q\|^2_{L^2(T)} \leq \|f_1\|^2_{L^2(T)} + \|f_2\|^2_{L^2(T)} \leq h_T^2 (1/8 + 1/j_{1,1}^2)(|f_1|^2_{H^1(T)} + |f_2|^2_{H^1(T)}).$$

Since ν_j is a unit vector,

$$|f_j|_{H^1(T)} = \|Dq \cdot \nu_j\|_{L^2(T)} \leq \|Dq\|_{L^2(T)} \, . \tag{5.1}$$

Hence,

$$|f_1|^2_{H^1(T)} + |f_2|^2_{H^1(T)} \leq 2 \, |q|^2_{H^1(T)} \, .$$

The combination with the aforementioned estimate of $\|q\|_{L^2(T)}$ proves the assertion. □

5.2. Raviart-Thomas finite element space

Given a regular triangulation $\mathcal{T}$ from Subsection 4.2, define the Raviart-Thomas finite element space

$$\begin{aligned} RT_0(\mathcal{T}) := \{q_{RT} \in P_1(\mathcal{T};\mathbb{R}^2) \cap H(\mathrm{div},\Omega) : \forall T \in \mathcal{T} \, \exists a_T, b_T, c_T \in \mathbb{R} \\ \forall x \in T, \, q_{RT}(x) = (a_T, b_T) + c_T(x_1, x_2)\}. \end{aligned}$$

It is well known that some piecewise polynomial function q_{RT} belongs to

$$H(\mathrm{div},\Omega) = \{q \in L^2(\Omega;\mathbb{R}^2) : \mathrm{div}\, q \in L^2(\Omega)\}$$

if and only if all the jumps $[q_{RT}]_E := (q_{RT}|_{T_+} - q_{RT}|_{T_-})|_E$, for $E = T_+ \cap T_-$ with $T_\pm \in \mathcal{T}$, across an interior edge E disappear in their normal component $[q_{RT}]_E \cdot \nu_E = 0$ along E. Given

an interior edge $E \in \mathcal{E}(T)$ shared by its neighbouring triangles T_+ and T_- and the vertices $P_\pm$ opposite to E of $T_\pm$, set

$$\Psi_E(x) := \begin{cases} \pm\frac{|E|}{2|T_\pm|}(x - P_\pm) & \text{for } x \in T_\pm, \\ 0 & \text{elsewhere.} \end{cases}$$

A corresponding formula without T_- applies to some boundary edge $E \in \mathcal{E}(\mathcal{T})$ with one neighbouring triangle T_+. Then $\Psi_E \in RT_0(\mathcal{T})$ with $\operatorname{supp}\Psi_E = \overline{w_E} := T_+ \cup T_-$ defines an edge-basis function of $RT_0(\mathcal{T})$. Indeed,

$$RT_0(\mathcal{T}) = \operatorname{span}\{\Psi_E : E \in \mathcal{E}\}.$$

The Fortin interpolation operator $I_F q$ is defined for all $q \in H^1(\Omega;\mathbb{R}^2)$ by

$$I_F q = \sum_{E\in\mathcal{E}} \left(\fint_E q \cdot \nu_E \, ds \right) \Psi_E$$

(with signs $\pm$ in the definition of $T_\pm$ and $\nu_E = \nu_{T_+}$) such that

$$(q - I_F q) \cdot \nu_E = 0 \text{ along any } E \in \mathcal{E}. \tag{5.2}$$

Theorem 5.2. *Let $q \in H^1(\Omega;\mathbb{R}^2)$ with Fortin interpolation $I_F q$. Then it holds*

$$\|q - I_F q\|_{L^2(\Omega)} \le C(\mathcal{T}) \, \|h_{\mathcal{T}} Dq\|_{L^2(\Omega)} .$$

Proof. The condition (5.2) leads to the assumption of Theorem 5.1 with q substituted by $q - I_F q$ on any triangle $T \in \mathcal{T}$. Theorem 5.1 shows

$$\|q - I_F q\|_{L^2(T)} \le C(\max \measuredangle T) h_T \, \|D(q - I_F q)\|_{L^2(T)} .$$

Any 2×2 matrix A with trace $\operatorname{tr}(A) = A_{11} + A_{22}$ and deviatoric part

$$\operatorname{dev} A = A - \operatorname{tr}(A)/2 \, I$$

allows for the orthogonality of the 2×2 unit matrix I and $\operatorname{dev} A$ with respect to the scalar product $A : B := \sum_{j,k=1,2} A_{jk} B_{jk}$ of the two matrices $A, B \in \mathbb{R}^{2\times 2}$. The Pythagoras theorem shows for the associated Frobenius norm $|\cdot|$ (i.e. $|A| = \sqrt{A : A}$)

$$|A|^2 = |\operatorname{dev} A|^2 + \operatorname{tr}(A)^2/2.$$

This identity for $A = D(q - I_F q)(x)$ followed by an integration of x over T leads to

$$\|D(q - I_F q)\|^2_{L^2(T)} = \|\operatorname{dev} D(q - I_F q)\|^2_{L^2(T)} + \|\operatorname{div}(q - I_F q)\|^2_{L^2(T)}/2.$$

Notice that $DI_F q|_T = c_T I$ for some $c_T \in \mathbb{R}$ is constant on T. Hence, $\operatorname{dev} DI_F q = 0$. Moreover, the Gauss divergence theorem and (5.2) show

$$\int_T \operatorname{div} q \, dx = \int_{\partial T} q \cdot \nu \, dx = \int_{\partial T} (I_F q) \cdot \nu \, ds = \int_T \operatorname{div}(I_F q) \, dx = 2c_T |T|.$$

Therefore, $\operatorname{div}(q - I_F q)$ has integral mean zero and so

$$\|\operatorname{div}(q - I_F q)\|_{L^2(T)} \le \|\operatorname{div} q\|_{L^2(T)} .$$

Altogether, and with another application of the Pythagoras theorem, it follows

$$\|D(q - I_F q)\|^2_{L^2(T)} \le \|\operatorname{dev} Dq\|^2_{L^2(T)} + \|\operatorname{div} q\|^2_{L^2(T)}/2 = \|Dq\|^2_{L^2(T)} .$$

The summation of the resulting estimate on $\|q - I_F q\|^2_{L^2(T)}$ over all $T \in \mathcal{T}$ concludes the proof. □

5.3. Raviart-Thomas MFEM

The mixed finite element method for the Poisson model problem of Subsection 4.1 with the Raviart-Thomas finite element space $RT_0(\mathcal{T})$ and the piecewise constant $P_0(\mathcal{T})$ seeks $(p_{RT}, u_{RT}) \in RT_0(\mathcal{T}) \times P_0(\mathcal{T})$ with

$$\begin{aligned} \int_\Omega p_{RT} \cdot q_{RT}\, dx + \int_\Omega u_{RT} \operatorname{div} q_{RT}\, dx = 0 \quad \text{for all } q_{RT} \in RT_0(\mathcal{T}); \\ \int_\Omega v_{RT} \operatorname{div} p_{RT}\, dx + \int_\Omega f v_{RT}\, dx = 0 \quad \text{for all } v_{RT} \in P_0(\mathcal{T}). \end{aligned} \tag{5.3}$$

Let $f_\mathcal{T}$ denote the piecewise L^2 projection of f onto $P_0(\mathcal{T})$ with

$$f_\mathcal{T}|_T := f_T := \fint_T f(x)\, dx \quad \text{for all } T \in \mathcal{T}. \tag{5.4}$$

Theorem 5.3. *There exists a unique solution (p_{RT}, u_{RT}) of the Raviart-Thomas MFEM. The discrete flux p_{RT} is the unique minimiser of*

$$\|p - q_{RT}\|_{L^2(\Omega)} \text{ for all } q_{RT} \in Q(f,\mathcal{T}) := \{q_{RT} \in RT_0(\mathcal{T}) : f_\mathcal{T} + \operatorname{div} q_{RT} = 0\}.$$

Proof. The existence of a unique solution follows from standard results in the theory of mixed FEM [1,6,18]. The optimality is well known and follows from (5.3) for the test function $q_{RT} := p_{RT} - r_{RT} \in Q(0,\mathcal{T})$ for any $r_{RT} \in Q(f,\mathcal{T})$. Indeed, (5.3) shows $p_{RT} \perp (p_{RT} - r_{RT})$. Since $p = \nabla u$ is a gradient, $(p - p_{RT}) \perp (p_{RT} - r_{RT})$ and so

$$\|p - r_{RT}\|^2_{L^2(\Omega)} = \|p - p_{RT}\|^2_{L^2(\Omega)} + \|p_{RT} - r_{RT}\|^2_{L^2(\Omega)}\,. \qquad \square$$

The following immediate consequence of Theorem 5.2 and 5.3 is announced as the a priori error estimate (1.3).

Corollary 5.1. *The Raviart-Thomas MFEM solution p_{RT} on Ω of the Poisson model problem* (4.1) *satisfies*

$$\|p - p_{RT}\|_{L^2(\Omega)} \le \|p - I_F p\|_{L^2(\Omega)} \le C(\mathcal{T})\, \|h_\mathcal{T} Dp\|_{L^2(\Omega)}\,.$$

Proof. The first inequality follows from the minimising property of Theorem 5.3 and the second from Theorem 5.2. $\square$

Remark 5.1. [Comparison with [7]] Corollary 5.1 is a significant improvement over [7]; the estimate [7, Equation (3.31)] is significantly greater than $C(\alpha)$.

5.4. Numerical example

Table 5.4 displays the errors $\|p - p_{RT}\|_{L^2(\Omega)}$, $\|p - I_F p\|_{L^2(\Omega)}$, and the efficiency index

$$EI := (C(\mathcal{T}_\ell)\, \|h_{\mathcal{T}_\ell} Dp\|_{L^2(\mathcal{T}_\ell)})/\|p - p_{RT}\|_{L^2(\Omega)}$$

for different levels ℓ in the benchmark problem from Subsection 4.4 based on the Matlab implementation [19].

Table 5.1: Numerical results for Raviart-Thomas MFEM.

ℓ	1	2	3	4	5
$\|p - p_{RT}\|_{L^2(\Omega)}$	0.98381972	0.56556947	0.29406962	0.14855355	0.07447061
$\|p - I_F p\|_{L^2(\Omega)}$	0.99628941	0.57150710	0.29503879	0.14868306	0.07448708
EI	4.99703932	4.34622629	4.17944042	4.13671187	4.12594455

6. Crouzeix-Raviart NCFEM

This section is devoted to the nonconforming finite element method (NCFEM) after Crouzeix and Raviart and its relation to the Raviart-Thomas MFEM usually associated with Marini [8]. The implications lead to some equivalence of error estimates for the two methods.

6.1. Crouzeix-Raviart NCFEM

The NCFEM after Crouzeix and Raviart concerns the nonconforming finite element space

$$V_{NC}(\mathcal{T}) := \{v \in P_1(\mathcal{T}) \,|\, v \text{ continuous at } \operatorname{mid}(\mathcal{E}), \text{ with } v = 0 \text{ for } \operatorname{mid}(\partial\Omega \cap \mathcal{E})\} \,.$$

The piecewise gradient $\nabla_{NC} : H^1(\mathcal{T}) \to L^2(\Omega;\mathbb{R}^2)$ is defined by $(\nabla_{NC} v)|_T := \nabla v|_T$ for all $T \in \mathcal{T}$ and defines the scalar product

$$a_{NC}(u,v) := \sum_{T\in\mathcal{T}} \int_T \nabla u \cdot \nabla v \, dx \quad \text{for all } u, v \in H^1(\mathcal{T})$$

and the induced discrete energy norm $|||\cdot|||_{NC} := \sqrt{a_{NC}(\cdot,\cdot)}$. For every $E \in \mathcal{E}$, the edge-oriented basis function ψ_E is defined by

$$\psi_E(\operatorname{mid}(E)) = 1 \text{ and } \psi_E(\operatorname{mid}(F)) = 0 \text{ for all } F \in \mathcal{E} \setminus \{E\}$$

and $V_{NC}(\mathcal{T}) = \operatorname{span}\{\psi_E \,|\, E \in \mathcal{E}(\Omega)\}$. The discrete Friedrichs inequality [6] reads

$$\|v\|_{L^2(\Omega)} \le C_{dF} |||v|||_{NC} \quad \text{for all } v \in V_{NC}(\mathcal{T}).$$

The constant C_{dF} does not depend on the mesh-size or cardinality of the shape-regular triangulation. The discrete Friedrichs inequality implies that $|||\cdot|||_{NC}$ is a norm on $V_{NC}(\mathcal{T})$ and the Riesz representation theorem guarantees a unique solution $u_{CR} \in V_{NC}$ of

$$a_{NC}(u_{CR}, v_{CR}) = \int_\Omega f v_{CR} \, dx \quad \text{for all } v_{CR} \in V_{NC}(\mathcal{T}). \tag{6.1}$$

6.2. Equivalence of CR-FEM and RT-MFEM

The following equivalence theorem is well known [8, 19] and is given here to stress that the right-hand side f in the Poisson model problem has to be modified to its piecewise integral mean $f_{\mathcal{T}} \in P_0(\mathcal{T})$ as in (5.4). For any $T \in \mathcal{T}$ set

$$s^2(T) := \sum_{E\in\mathcal{E}(T)} |E|^2 = 36 \, \|\bullet - \operatorname{mid}(T)\|_{L^2(T)} / \, |T| \,.$$

The following theorem states a representation of the unique solution (5.3).

Theorem 6.1 (Marini [8]) *Suppose that $\tilde{u}_{CR} \in V_{NC}(\mathcal{T})$ solves the discrete problem for the Crouzeix-Raviart FEM with modified right-hand side $f_{\mathcal{T}} \in P_0(\mathcal{T})$, i.e., $\tilde{u}_{CR} \in V_{NC}(\mathcal{T})$ satisfies*

$$a_{NC}(\tilde{u}_{CR}, v_{CR}) = \int_\Omega f_{\mathcal{T}} v_{CR}\, dx \quad \text{for all } v_{CR} \in V_{NC}(\mathcal{T}). \tag{6.2}$$

Then the solution (p_{RT}, u_{RT}) of (5.3) reads

$$p_{RT}(x) = \nabla_{NC}\tilde{u}_{CR} - f_T/2\ (x - \mathrm{mid}(T)) \quad \text{for } x \in T \in \mathcal{T},$$
$$u_{RT} = \fint_T \tilde{u}_{CR}\, dx + s^2(T) f_T/144 \quad \text{on } T \in \mathcal{T}. \qquad \square$$

6.3. CR-FEM error estimate

This section establishes the error estimate (1.4) for the Crouzeix-Raviart nonconforming finite element method. The oscillations of a function $f \in L^2(\Omega)$ are defined as

$$\mathrm{osc}(f, \mathcal{T})^2 := \sum_{T \in \mathcal{T}} h_T^2 \left\| f - f_T \right\|_{L^2(T)}^2.$$

Theorem 6.2. *The Crouzeix-Raviart NCFEM solution $u_{CR} \in V_{NC}(\mathcal{T})$ on Ω of the Poisson model problem (4.1) satisfies*

$$\left|\!\left|\!\left| u - u_{CR} \right|\!\right|\!\right|_{NC} \le \frac{1}{j_{1,1}} \mathrm{osc}(f, \mathcal{T}) + \sqrt{\frac{1}{j_{1,1}^2} + C(\mathcal{T})^2}\, \left\| h_{\mathcal{T}} D^2 u \right\|_{L^2(\Omega)}.$$

Proof. Let $\tilde{u}_{CR} \in V_{NC}(\mathcal{T})$ solve (6.2) and set $\tilde{p}_{CR} := \nabla_{NC}\tilde{u}_{CR} \in P_0(\mathcal{T}; \mathbb{R}^2)$. The orthogonality of the L^2 projection Π_0 onto $P_0(\mathcal{T})$ plus the Poincaré inequality show

$$\begin{aligned}
\left|\!\left|\!\left| \tilde{u}_{CR} - u_{CR} \right|\!\right|\!\right|_{NC}^2 &= a_{NC}(\tilde{u}_{CR}, \tilde{u}_{CR} - u_{CR}) - a_{NC}(u_{CR}, \tilde{u}_{CR} - u_{CR}) \\
&= \int_\Omega (f - f_{\mathcal{T}})(\tilde{u}_{CR} - u_{CR}) dx \\
&= \int_\Omega (f - f_{\mathcal{T}})\big((\tilde{u}_{CR} - u_{CR}) - \Pi_0(\tilde{u}_{CR} - u_{CR})\big) dx \\
&\le \frac{1}{j_{1,1}} \mathrm{osc}(f, \mathcal{T}) \left|\!\left|\!\left| \tilde{u}_{CR} - u_{CR} \right|\!\right|\!\right|_{NC}.
\end{aligned}$$

Hence, $\left|\!\left|\!\left| \tilde{u}_{CR} - u_{CR} \right|\!\right|\!\right|_{NC} \le \mathrm{osc}(f, \mathcal{T})/j_{1,1}$. The Pythagoras theorem leads to

$$\left\| p - \tilde{p}_{CR} \right\|_{L^2(\Omega)}^2 = \left\| p - \Pi_0 p \right\|_{L^2(\Omega)}^2 + \left\| \Pi_0 p - \tilde{p}_{CR} \right\|_{L^2(\Omega)}^2.$$

For the first term on the right-hand side, the Poincaré inequality yields

$$\left\| p - \Pi_0 p \right\|_{L^2(\Omega)}^2 \le \frac{1}{j_{1,1}^2} \left\| h_{\mathcal{T}} D p \right\|_{L^2(\Omega)}^2.$$

For the second term, Theorem 6.1 leads to $\Pi_0 p_{RT} = \tilde{p}_{CR}$ and therefore

$$\left\| \Pi_0 p - \tilde{p}_{CR} \right\|_{L^2(\Omega)}^2 = \left\| \Pi_0 (p - p_{RT}) \right\|_{L^2(\Omega)}^2 \le \left\| p - p_{RT} \right\|_{L^2(\Omega)}^2.$$

Thus, Corollary 5.1 and the triangle inequality conclude the proof. $\square$

Remark 6.1. The estimate in [7, Theorem 4.1] is wrong in the sense that the difference of u_{CR} and $\tilde{u}_{CR}$ has been neglected. Even the corrected version of that estimate is less sharp than Theorem 6.2 because of Remark 5.1.

6.4. Numerical example

Table 6.4 displays the error $|||u-u_{CR}|||_{NC}$, the oscillations $\mathrm{osc}(f,\mathcal{T})$, and the efficiency index

$$EI := \left(\frac{1}{j_{1,1}}\,\mathrm{osc}(f,\mathcal{T}) + \sqrt{\frac{1}{j_{1,1}^2}+C(\mathcal{T})^2}\,\left\|h_{\mathcal{T}}D^2u\right\|_{L^2(\Omega)}\right)/|||u-u_{CR}|||_{NC}$$

in the benchmark problem from Subsection 4.4.

Table 6.1: Numerical results of Crouzeix-Raviart FEM.

ℓ	1	2	3	4	5
$\|\|\|u-u_{CR}\|\|\|_{NC}$	1.34051563	0.73261164	0.37526998	0.18881556	0.09455757
$\mathrm{osc}(f,\mathcal{T})$	1.97765293	0.53229065	0.13533651	0.03397415	0.00850227
EI	4.36265775	3.82871143	3.64628361	3.57691331	3.54782899

Acknowledgments. The authors would like to thank the two anonymous referees for their valuable comments and suggestions. In particular, to the second referee which pointed us to the recently improved Poincaré constant for triangles. This research was supported by the World Class University (WCU) program through the National Research Foundation of Korea (NRF) funded by the Ministry of Education, Science and Technology R31-2008-000-10049-0 and the DFG Research Center MATHEON "Mathematics for key technologies" in Berlin. The second author was supported in parts by the DFG graduate school BMS "Berlin Mathematical School".

References

[1] D. Braess, Finite elements, Cambridge University Press, Cambridge, second edition, 2001, Theory, fast solvers, and applications in solid mechanics, Translated from the 1992 German edition by Larry L. Schumaker.

[2] P.G. Ciarlet, The finite element method for elliptic problems, volume 4 of *Studies in Mathematics and its Applications*, North-Holland Publishing Co., Amsterdam, 1978.

[3] F. Kikuchi and X. Liu, Estimation of interpolation error constants for the P_0 and P_1 triangular finite elements, *Comput. Methods Appl. Mech. Engrg.*, **196**:37-40 (2007), 3750–3758.

[4] I. Babuška and A.K. Aziz, On the angle condition in the finite element method, *SIAM J. Numer. Anal.*, **13**:2 (1976), 214–226.

[5] G. Acosta and R.G. Durán, The maximum angle condition for mixed and nonconforming elements: application to the Stokes equations, *SIAM J. Numer. Anal.*, **37**:1 (1999), 18–36.

[6] S.C. Brenner and L.R. Scott, The mathematical theory of finite element methods, volume 15 of *Texts in Applied Mathematics*, Springer, New York, third edition, 2008.

[7] S. Mao and Z. Shi, Explicit error estimates for mixed and nonconforming finite elements, *J. Comput. Math.*, **27**:4 (2009), 425–440.

[8] L.D. Marini, An inexpensive method for the evaluation of the solution of the lowest order Raviart-Thomas mixed method, *SIAM J. Numer. Anal.*, **22**:3 (1985), 493–496.

[9] D.N. Arnold and F. Brezzi, Mixed and nonconforming finite element methods: implementation, postprocessing and error estimates, *RAIRO Modél. Math. Anal. Numér.*, **19**:1 (1985), 7–32.

[10] L.E. Payne and H.F. Weinberger, An optimal Poincaré inequality for convex domains, *Arch. Rational Mech. Anal.*, **5** (1960), 286–292.

[11] R.S. Laugesen and B.A. Siudeja, Minimizing Neumann fundamental tones of triangles: an optimal Poincaré inequality, *J. Differential Equations*, **249**:1 (2010), 118–135.

[12] P. Arbenz, Computable finite element error bounds for Poisson's equation, *IMA J. Numer. Anal.*, **2**:4 (1982), 475–479.

[13] R. Lehmann, Computable error bounds in the finite-element method, *IMA J. Numer. Anal.*, **6**:3 (1986), 265–271.

[14] G.L. Siganevich, The best error estimate for linear interpolation on a triangle of functions in $W_2^2(T)$, *Dokl. Akad. Nauk SSSR*, **300**:4 (1988), 811–814.

[15] L.C. Evans, Partial differential equations, volume 19 of *Graduate Studies in Mathematics*, American Mathematical Society, Providence, second edition, 2010.

[16] D. Gilbarg and N.S. Trudinger, Elliptic partial differential equations of second order, Classics in Mathematics, Springer, Berlin, 2001, Reprint of the 1998 edition.

[17] J. Alberty, C. Carstensen and S.A. Funken, Remarks around 50 lines of Matlab: short finite element implementation, *Numer. Algorithms*, **20**:2-3 (1999), 117–137.

[18] F. Brezzi and M. Fortin, Mixed and hybrid finite element methods, volume 15 of *Springer Series in Computational Mathematics*, Springer, New York, 1991.

[19] C. Bahriawati and C. Carstensen, Three MATLAB implementations of the lowest-order Raviart-Thomas MFEM with a posteriori error control, *Comput. Methods Appl. Math.*, **5**:4 (2005), 333–361.